

## Absorption and reflection of infrared radiation by polymers in fire-like environments

Gregory Linteris<sup>1,\*</sup>, Mauro Zammarano<sup>1</sup>, Boris Wilthan<sup>2</sup> and Leonard Hanssen<sup>2</sup>

<sup>1</sup>*Fire Science Division, National Institute of Standards and Technology, Gaithersburg, MD, USA*

<sup>2</sup>*Optical Technology Division, National Institute of Standards and Technology, Gaithersburg, MD, USA*

### SUMMARY

In large-scale fires, the input of energy to burning materials occurs predominantly by radiative transfer. The in-depth (rather than just surface) absorption of radiant energy by a polymer influences its ignition time and burning rate. The present investigation examines two methods for obtaining the absorption coefficient of polymers for infrared radiation from high-temperature sources: a broadband method and a spectral method. Data on the total average broadband transmittance for 11 thermoplastics are presented (as are reflectance data), and the absorption coefficient is found to vary with thickness. Implications for modeling of mass loss experiments are discussed. Copyright © 2011 John Wiley & Sons, Ltd.

Received 3 March 2011; Revised 6 June 2011; Accepted 9 June 2011

KEY WORDS: pyrolysis modeling; material flammability; IR absorption; polymer diathermicity; thin-film glazings

### 1. INTRODUCTION

The absorption of radiation in semi-transparent media is a complex but well-studied phenomena [1]. In-depth absorption of radiation has applications to ablative materials for reentry bodies and hypersonic vehicles [2], thermoforming and processing of polymers [3–6], thin-film glazing for solar thermal systems [7], and prediction of polymer burning rates in fires [8–10].

In fire research, the in-depth absorption of radiation is important for material ignition as well as for fire growth and spread [11]. When subjected to a known radiant flux, the polymer's time to ignition and subsequent mass loss rate are controlled primarily by the material's thermodynamic and chemical kinetic properties related to decomposition, as well as by those related to the transfer of heat into the material (such as the density, thermal conductivity, and specific heat) [12]. For semi-transparent materials, in-depth absorption of radiation, diathermicity, is also important [13]. Moreover, accurate knowledge of the absorption of the radiation is required for the validation of models of material decomposition [14,15].

Recently, the in-depth absorption of radiation has been shown to have a large effect on the time to ignition for poly(methyl methacrylate) (black PMMA) subjected to a high ( $>100\text{kW m}^{-2}$ ) radiant flux [16]. In that reference, Jiang *et al.* measured the absorption coefficient of black PMMA with a broadband source and detector and developed an analytical model for predicting the ignition time. The model was able to predict well the ignition time measured in earlier experiments [17]. Bal and Rein [18] extended the work of Jiang *et al.* to consider the possibility of other parameters affecting the ignition time at high flux but again showed that it is influenced mainly by in-depth absorption. In a

\*Correspondence to: Gregory Linteris, Fire Science Division, National Institute of Standards and Technology, Gaithersburg, MD, USA.

†E-mail: linteris@NIST.GOV

related work, differences in the pyrolysis behavior induced by a cone heater or the FM Global Fire Propagation Apparatus (FPA) are discussed [19].

Recently, the effect of infrared (IR) transmission in a polymer on the time to ignition has been calculated for a polymer slab (PMMA), of varying decomposition rates and absorption coefficients, subjected to varying radiant fluxes [20]. For example, Figure 1 shows the ignition time for a 25.4-mm-thick slab of PMMA as a function of the imposed radiant flux, with total average (integrated over all wavelengths) absorption coefficient varied from 200 to 50,000  $\text{m}^{-1}$  [20]. As indicated, this variation in the absorption coefficient gives a factor of 2 difference in the ignition time at low flux and 11 at high flux. In addition to the ignition time, the burning characteristics of the PMMA are changed as well, so that for model validation, the value of the absorption coefficient can be important [20].

The goal of the present work is to examine several methods of obtaining the required average absorption coefficient for polymers exposed to the radiant flux typical of fires, so that the value of that parameter can be inputted into numerical models of fire growth, such as the Fire Dynamics Simulator [21], GPyro [12], or ThermaKin [22]. As described below, two methods were used to study the absorption of IR by thermoplastic polymers. The first is based on the National Institute of Standards and Technology (NIST) gasification device (GD) [23], and the second, on the NIST integrating-sphere (IS) system with a Fourier transform spectrophotometer [24].

## 2. EXPERIMENT

### 2.1. National Institute of Standards and Technology gasification device

The NIST GD has been described previously [23]. In the present work, a cone-shaped resistive heater at  $(1081 \pm 1)\text{K}$  and located in a water-cooled, nitrogen-purged chamber irradiates the horizontal polymer specimen located 14 cm from the heater bottom. The  $50\text{mm} \times 50\text{mm}$  polymer sheets are placed horizontally and centered on top of a vertical stainless steel tube (diameter 2.54 cm). Concentric in the tube and located 1 cm below the polymer sample is a calibrated heat flux gage (Medterm Corp., Huntsville, AL, model GTW-732-485A)<sup>1</sup>, which monitors the broadband radiation transmitted through the sample. A water-cooled shutter, positioned between the cone heater and the sample, blocks radiation until a test is initiated, whereupon the shutter is removed, and the data are collected for about 5 s, and the shutter is replaced. The measurements in the NIST GD are performed using an approach similar to that in reference [16]; however, the NIST device does not attempt to conductively cool the sample.

### 2.2. Integrating-sphere device

The NIST IS device has been described previously [24]. A modulated beam from a Fourier transform infrared spectrometer (FTIR) passes through the material, which is mounted on the sample port of an integrating sphere. A HgCdTe detector with a non-imaging concentrator, also mounted on the integrating sphere, monitors either the reflected or transmitted energy through the sample, and a ratio to the reference beam through the empty reference port of the sphere is computed [25]. The value of the spectral transmittance  $\tau_\lambda$ , or spectral reflectance  $\rho_\lambda$ , for the sample of thickness  $S$ , is measured directly for wavelengths within the sensitivity of the detector (1.5 to 15.1  $\mu\text{m}$ ). Although both the total and specular components of the transmitted and reflected light are obtained (the specular component can be computed from measured data), only the total of the near normal ( $8^\circ$ ) directional hemispherical reflectance/transmittance values are reported in the present work for comparison with the results obtained using the NIST GD.

### 2.3. Terminology

It is of value to provide a summary of the various terms used in the present work. Following the descriptions in Siegel and Howell [1], the absorption coefficient,  $a$  (in  $\text{m}^{-1}$ ), is the property of a

<sup>1</sup>Certain commercial equipment, instruments, and materials are identified in this paper to adequately specify the procedure. Such identification does not imply recommendation or endorsement by the National Institute of Standards and Technology.

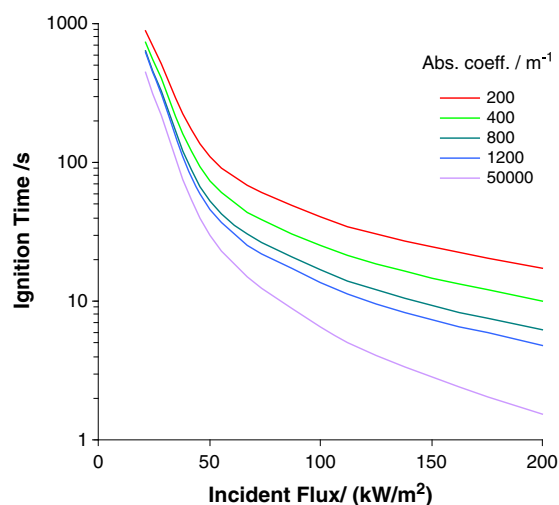


Figure 1. Ignition time as a function of the radiant flux, for a 25.4-mm-thick sample of poly(methyl methacrylate) with varying values of the absorption coefficient (from [20]).

medium that quantifies the absorption of thermal radiation per unit path length within the medium, while the absorptance  $\alpha$  (dimensionless) quantifies the fraction of radiant energy traveling along a path that will be absorbed within a given distance  $\alpha = (1 - e^{-aS})$ , in which  $S$  is the path length through the medium. The similar term absorptivity  $\alpha$  (dimensionless) is a property of a material that gives the fraction of incident energy on the material that is absorbed. That is, the absorptivity is a surface property of an opaque material (one filling half of all space), and  $\alpha = 1 - \rho$ , where  $\rho$  is the reflectivity. Similarly, reflectivity and reflectance (both dimensionless) are a measure of the fraction of all incident energy that will be reflected at an interface between two materials; reflectivity refers to that occurring from a material filling half of all space, whereas reflectance refers to a material of a given thickness.

#### 2.4. Materials

Ten typical commodity polymers were used, from the same sample batch, and provided by the authors of references [16,26,27]: black poly(methyl methacrylate), black PMMA (Polycast PMMA, Spartech Plastics, Clayton, MO); poly(methyl methacrylate), PMMA; poly(oxymethylene) (copolymer), POM; polyethylene (high density), HDPE; polypropylene, PP; polystyrene (high impact), HIPS; polyamide 6,6, PA66; poly(ethylene terephthalate), PET; poly(butylene terephthalate), PBT; and PBT with glass fiber, PBT-GF. In addition, polystyrene, PS (Styron 666D, Dow Chemical Company, Midland, MI), was tested. The samples were prepared by hot pressing to the desired thickness. The actual thickness of all the samples was subsequently determined as the average of five measurements with a micrometer in the central region, corresponding to the optical path.

#### 2.5. Uncertainties

All uncertainties are reported as *expanded uncertainties*  $ku_c$ , from a combined standard uncertainty (estimated standard deviation)  $u_c$  and a coverage factor  $k$  as described. Likewise, when reported, the relative uncertainty is  $ku_c/X$ . The only measured parameters are the material thickness and the transmitted and reflected (in the case of the IS) intensity. The uncertainty (type B) in the thickness arises primarily from variation in the material thickness in the region of the measurement. In the central (diameter 6mm) portion of the samples where the transmission measurements were taken, the relative uncertainty (66% confidence level,  $k=1$ ) was typically  $<2\%$  for all thicknesses of all polymers. Exceptions to this were the polymers HIPS, PBT, PMMA, PET, and POM, which were  $<3\%$ , as well as the specific samples listed in Table I, which had the relative uncertainties as noted.

In the NIST GD, the combined relative uncertainty (type B) on the transmittance is estimated to be 5% ( $k=2$ ), mostly from correction for the polymer re-radiation, as described in the Section 4. In the NIST IS device, the combined relative uncertainty ( $k=2$ ) for the spectral transmittance or reflectance

Table I. Uncertainties in select measured polymer thicknesses.

Polymer	Thickness (mm)	
PA66	0.069	±0.004
PMMA (black)	0.093	±0.008
	0.108	±0.006
	0.174	±0.010
HDPE	0.420	±0.060
PP	0.061	±0.006
HIPS	0.080	±0.005
	0.470	±0.028
PMMA	0.506	±0.028
	0.941	±0.062
POM	0.465	±0.051

varies between 0.3% for specular samples (PET, HDPE, PMMA, and PBT) and 3% for diffuse samples (the degree of specularity varies with material type, thickness, and wavelength).

### 3. DATA ANALYSIS

The attenuation of radiation within a medium is described by Bouguer's law:

$$\frac{i'_{\lambda}(S)}{i'_{\lambda}(0)} = \exp \left[ \int_0^S K_{\lambda}(S^*) dS^* \right] \quad (1)$$

in which  $i$  is the radiation intensity,  $K$  is the extinction coefficient,  $S$  is the path length through the medium, and the subscript  $\lambda$  and superscript  $'$  denote spectral and directional [1]. The extinction coefficient is composed of two parts, an absorption coefficient  $a_{\lambda}(\lambda)$  and a scattering coefficient  $\sigma_{s,\lambda}(\lambda)$ :

$$K_{\lambda} = a_{\lambda}(\lambda) + \sigma_{s,\lambda}(\lambda) \quad (2)$$

The inverse of the extinction coefficient is the mean penetration depth of the radiation ( $l_m = 1/K_{\lambda}$ ). For the present conditions, the scattered light is assumed to be quickly absorbed, so that  $K_{\lambda} \approx a_{\lambda}$ , and assuming isotropic behavior,  $a_{\lambda}$  does not vary with  $S$ , so Bouguer's law becomes

$$\tau'_{\lambda}(S) = \frac{i'_{\lambda}(S)}{i'_{\lambda}(0)} = e^{-a_{\lambda}S} \quad (3)$$

in which  $\tau'_{\lambda}(S)$  is the directional spectral transmittance for the path length  $S$ .

Ultimately, a value for the absorption coefficient,  $a$ , is desired, which is an average (over all wavelengths) and a total (sum of directional and diffuse), because this is what is used to describe radiation transport in common sub-grid models for material decomposition in fires [12,21,22]. In the transmission experiments using the cone heater in the NIST gasification device, the incident radiation is spectrally broad and is assumed to follow a blackbody distribution at the heater temperature. Hence, the measurements represent the average (not spectral) transmittance  $\tau'(S)$ . Also, the configuration does not distinguish between the diffuse and specular components of the transmitted radiation. As a result, the NIST GD measures the average total transmittance  $\tau(S)$ , from which the average total absorption coefficient  $a$  can be determined. For a very thin sample, with the inclusion of the front and back reflective surfaces (and neglecting the effects of multiple reflections), the transmission of light through a thin sheet of material becomes

$$I/I_0 = (1 - \rho)^2 \tau(S) = (1 - \rho)^2 e^{-aS} \tag{4}$$

in which  $\rho$  is the average total reflectivity of each surface,  $I$  is the average total intensity after passing through the material of the thickness  $S$ , and  $I_0$  is the average total intensity prior to interaction with the material (i.e., before the first surface reflection). This can be rewritten as

$$\ln(I/I_0) = 2\ln[(1 - \rho)] - aS \tag{5}$$

so that a plot of  $-\ln(I/I_0)$  versus  $S$  has a slope of  $a$  and an intercept of  $-2\ln[1 - \rho]$ .

In the case of the NIST IS, the directional (or total) spectral transmittance  $\tau'_\lambda(\lambda)$  is measured directly for a given thickness of material. To obtain the average total absorption coefficient  $a$  from the measurements in the IS, the spectral transmittance is averaged over the conditions of the measurements in the NIST GD (with which we will compare the IS measurements). Hence, we use the IS-measured total spectral transmittance  $\tau_\lambda(\lambda, S)$  and average this over the spectral distribution of the incident radiation from the conically shaped radiant heater in the NIST GD. The average total transmittance  $\tau(S)$  for a sample of thickness  $S$  is then given by

$$\tau(S) = \frac{\int_0^\infty \tau_\lambda(\lambda, S) i'_\lambda(0) d\lambda}{\int_0^\infty i'_\lambda(0) d\lambda} \tag{6}$$

in which the incident spectral radiation intensity  $i'_\lambda(0)$  is approximated as that of a black body in a vacuum at the measured heater temperature. Using Planck's spectral distribution

$$i'_\lambda(0) = i'_{\lambda_b}(\lambda) = \frac{2C}{\lambda^5 (e^{C_2/\lambda T} - 1)} \tag{7}$$

(with  $C_1 = 0.59544 \times 10^{-16} \text{ W m}^2$  and  $C_2 = 14,388 \mu\text{m K}$  [1]) provides  $\tau(S)$ , and the resulting data can be plotted as  $-\ln[\tau(S)]$  versus  $S$  to yield  $a$  as the slope.

The reflectance can also be illustrated via the plots of  $-\ln(I/I_0)$  versus  $S$ . That is, as indicated above, the intercept of the curve (i.e., zero thickness) is  $-2\ln(1 - \rho)$ . In the IS measurements, the diffuse, directional, and total reflectance are obtained for each sample thickness of each of the 11 polymers. To calculate the average total reflectance  $\rho(S)$ , we substituted the total spectral reflectance  $\rho_\lambda(\lambda, S)$  for the total spectral transmittance  $\tau_\lambda(\lambda)$  in Equation 6. For these polymer films, the normal incidence average total reflectance  $\rho$  can also be estimated [7] based on the real part of the index of refraction in the visible ( $n_f$ ):

$$\rho = \left( \frac{n_f - 1}{n_f + 1} \right)^2 \tag{8}$$

#### 4. RESULTS AND DISCUSSION

For the NIST GD, typical time traces of the measured heat flux through four thicknesses of POM are shown in Figure 2. In that figure, the incident heat flux (in the absence of polymer sample) is  $35.8 \text{ kW m}^{-2}$ . As indicated, after the shutter is removed and the flux-gage transient occurs (about 1 s), the flux increases with time (because of absorption of radiation, polymer heating, and subsequent re-radiation); the effect is larger for thinner samples (which heat faster). In the data analysis, the value of the transmitted flux in the absence of polymer heating is obtained by extrapolating the increasing flux back (three points) to the time where the shutter is removed (as indicated near the rising part of the curve for  $S=0.37$  in Figure 2). The uncertainty in this value is estimated to be one-half the correction because of the extrapolation.

From the gasification device experimental data of Figure 2, a plot of  $-\ln(I/I_0)$  versus the thickness of the POM samples is generated ( $\Delta$  symbols), as shown in Figure 3. Note that the uncertainties in the

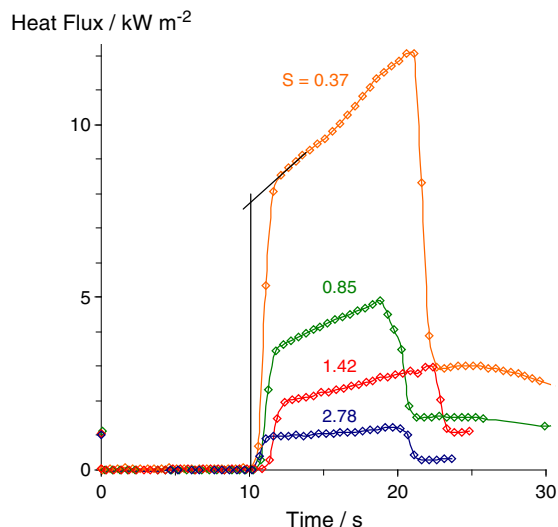


Figure 2. Time history of heat flux through the back face of poly(oxymethylene) (POM) (for four sample thicknesses), with the front face exposed to an incident flux of  $35.8\text{ kW m}^{-2}$ .

thickness and  $-\ln(I/I_0)$  are smaller than the symbol size. (Note that the relevant intensities in the expression  $I/I_0$  are before and after the front and back surfaces, so the effects of surface reflections on  $I/I_0$  will appear in the figures.) The slope of this line gives the average (integrated over all wavelengths) absorption coefficient  $a$  for the material (POM) for incident radiation with a power distribution given by a blackbody at the source temperature of NIST GD (1081 K). As indicated,  $-\ln(I/I_0)$  versus  $S$  is not linear, so the absorption coefficient is not a constant. As indicated in the figure, the slope varies by a factor of nearly 4 for the range of thicknesses of the measurements. This is in contrast to the data of Jiang *et al.* [16] for black PMMA, in which measurements over a range of thicknesses from 1 to 3.8 mm show a constant slope ( $a$ ). The two points at the value of  $S=0$  correspond to attenuation from surfaces reflections,  $-\ln(I/I_0) = -2\ln(1 - \rho)$ , with the value of  $\rho$  given from the IS measurement ( $\circ$  symbol) or using the real part of the index of refraction (for visible light),  $n_f=1.48$  for POM ( $\diamond$  symbol). As indicated, these values agree well with each other for the present tests. The dotted lines in the figure give the *apparent* value of the absorption coefficient that one would obtain from a single measurement of the average total transmittance through either a 0.37-mm or a 2.9-mm-thick slab of POM (using the values of the reflectance as obtained as described above); these values are  $3550$  and  $1250\text{ m}^{-1}$ , respectively. Also shown in Figure 3 (right scale) is the

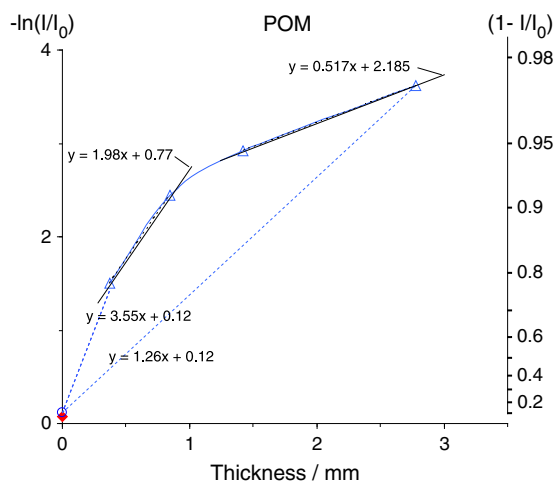


Figure 3.  $-\ln(I/I_0)$  versus thickness for poly(oxymethylene) (POM) (National Institute of Standards and Technology gasification device).

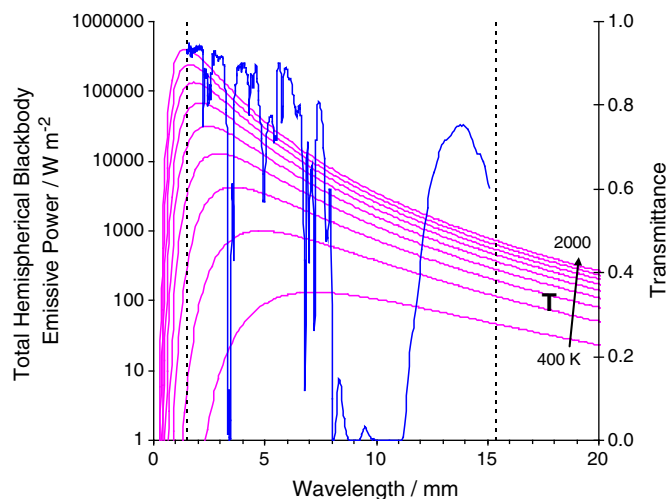


Figure 4. Blackbody hemispherical emissive power as a function of wavelength, for source temperatures of 400 to 2000 K (left scale), together with transmittance (right scale) for poly(oxymethylene) ( $S=0.027$  mm).

fraction of incident energy absorbed  $[1 - (I/I_0)]$  at each thickness (which allows a better physical interpretation than  $-\ln(I/I_0)$ ). As indicated, for POM, about three-fourths of the energy is absorbed within the first  $1/3$  mm; hence, most of the energy absorption occurs at the value of the apparent value of  $a$ , which is quite high ( $3500 \text{ m}^{-1}$ ).

To explore the non-linear behavior in Figure 3 for POM in more detail, we present the results of measurements in the IS. Figure 4 shows the total spectral transmittance  $\tau_\lambda(\lambda, S)$  for POM ( $S=0.027$  mm; right scale) as a function of wavelength; also shown (left scale) is the blackbody hemispherical emissive power,  $e_{\lambda_b}(\lambda)$  (note the semi-log scale, and note that  $e_{\lambda_b}(\lambda) = \pi i'_{\lambda_b}(\lambda)$ ), for source temperatures from 400 to 2000 K. The IS data are shown for the wavelength range of the instrument ( $1.5$  to  $15.1 \mu\text{m}$ )<sup>2</sup>.

From the data in Figure 4, the total average transmittance  $\tau(S)$  is calculated using Equation 6, assuming a blackbody source temperature the same as the heater in the NIST GD (1081 K). Figure 5 shows  $-\ln(I/I_0)$  in the NIST GD ( $\Delta$  symbols, left scale) together with the results in the NIST IS ( $\bullet$  symbols, left scale). As indicated, the agreement between the two methods is excellent for this polymer (and this range of integration of the spectral transmittance). Hence,  $-\ln(I/I_0)$  as measured with the IS also varies non-linearly with  $S$ .

In order to demonstrate the effect of the spectral range of the instrument on the results, we also calculated the transmittance (and reflectance) for a smaller spectral range, from  $2.5$  to  $15.1 \mu\text{m}$  (selected because it is a common range of current FTIRs and has been used in the past by other researchers [7], whose results have been adopted by others [15]). In Figure 5,  $-\ln(I/I_0)$  is shown as a function of  $S$ , for the smaller spectral range. As indicated, for the narrower spectral range, the curve for  $-\ln(I/I_0)$  is more nearly linear, with a slope closer to the thin sample results. Consequently, using the  $2.5$ - $\mu\text{m}$  to  $15.1$ - $\mu\text{m}$  range produces a result that is both qualitatively and quantitatively different from the  $1.5$ - $\mu\text{m}$  to  $15.1$ - $\mu\text{m}$  results.

In order to more fully explore possible non-Bouguer's law absorption behavior by common polymers used in materials fire research, we also examine the absorption and reflection of IR by black Polycast PMMA. This material is selected because it is nearly a standard material in cone-calorimeter studies and was recently used by Jiang *et al.* [16] to study the effects of diathermicity on ignition behavior at high flux. In addition to the development and application of an analytic model for predicting the ignition of materials with in-depth absorption of energy, Jiang *et al.* also measured the transmission of broadband IR through black Polycast PMMA of four thicknesses and used these to determine the broadband absorption coefficient. The IR heaters of the FM Global FPA were used, in a

<sup>2</sup>The raw data for the spectral transmission and absorption are available from the author upon request.

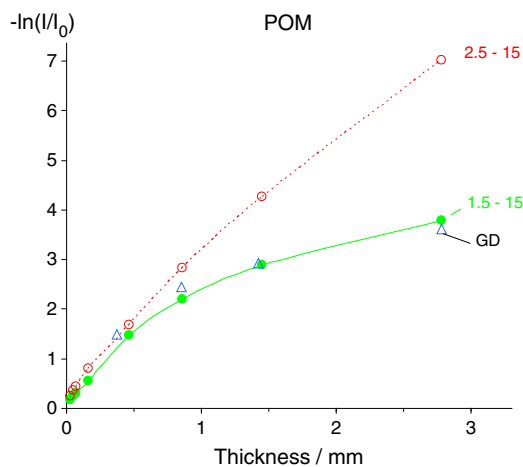


Figure 5.  $-\ln(I/I_0)$  versus thickness for poly(oxymethylene) (POM) ( $\Delta$ : gasification device (GD) and  $\circ$ : integrating sphere).

range of color temperatures from 1050 to 1650 K, which was changed by varying the input voltage to the heaters. The broadband energy transmitted through the samples (thickness  $\approx$  1 mm to 4 mm) was detected with a calibrated heat flux gage.

For comparison with their results, we obtained samples of the Polycast black PMMA (same lot) from the authors of reference [16]. We pressed them into varying thicknesses (0.090 to 3.00 mm) and measured the transmission and reflection of radiation using both the NIST GD and the NIST IS. Data were analyzed using the methods described above, and the results are presented in Figure 6. The data in reference [16] are shown ( $-$  and  $-$  symbols, for source temperatures of 1650 and 1050 K, respectively), with a curve fit (solid line) to the data from all source temperatures. As indicated, the inferred absorption coefficient is  $960.5 \text{ m}^{-1}$  (and there was little variation with source temperature [16]). The data in the present work, taken in the NIST GD, are shown by the open triangles. Also shown in the figure are the data from the NIST IS, with the transmission spectrum integrated for a blackbody temperature of 1081 K and a wavelength range of 1.5 to  $15.1 \mu\text{m}$  ( $\bullet$  symbols). (For comparison, data are also shown ( $\circ$  symbols) in which the IS values of  $\tau_\lambda(\lambda, S)$  were converted to the average total transmittance  $\tau(S)$  for a source temperature of 1650 K, to allow comparison with the higher temperature source temperatures in reference [16].)

For the black PMMA, the agreement between the NIST GD and the NIST IS data is excellent (as was the case for POM). As indicated, for the range of material thickness tested by Jiang *et al.* (1 to 3 mm), the

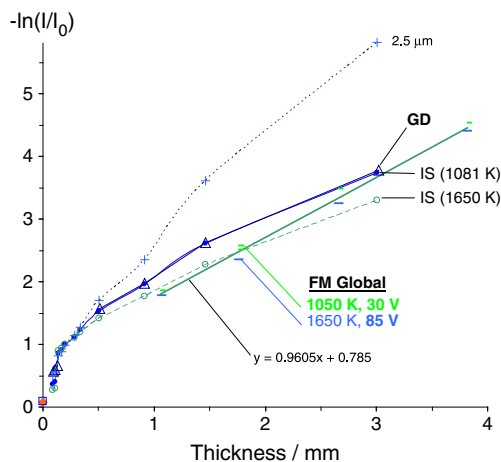


Figure 6.  $-\ln(I/I_0)$  versus thickness for black Polycast poly(methyl methacrylate) as measured at the National Institute of Standards and Technology ( $\Delta$ ,  $\bullet$ , and  $+$  symbols) and at FM Global [16] ( $-$  and  $-$  symbols). GD, gasification device; IS, integrating sphere.

slope implied by the NIST data (about  $830\text{m}^{-1}$ ) is close to that of reference [16],  $960.5\text{m}^{-1}$  (although there is a slight offset in the data). Use of the higher source temperature to define the power distribution of the incident radiation over which to integrate the IS spectral data produces the lower IS curve ( $\circ$  symbols) in Figure 6. The data are very close in magnitude to those of reference [16], and although the slope is slightly different ( $a=720\text{m}^{-1}$ ), the agreement is not unreasonable given the approximations made throughout. Analysis of the IS data was also performed for a range of integration from  $2.5$  to  $15.1\mu\text{m}$ , with a source temperature of  $1081\text{K}$  (as indicated by the  $+$  symbols in Figure 6 in the curve labeled ' $2.5\mu\text{m}$ '); as with POM, for this narrower wavelength range, the results are significantly different from the results for the  $1.5\mu\text{m}$  to  $15.1\mu\text{m}$  spectral range, especially for the larger thicknesses.

Most striking about the data in Figure 6 for black PMMA is that (as was found for POM) the plot of  $-\ln(I/I_0)$  versus  $S$  is non-linear, especially at the smaller thicknesses. To illustrate this effect, Figure 7 shows, for black PMMA, the variation with thickness in the absorption coefficient (i.e., the slope in Figure 6) for broadband IR as calculated using the data from the NIST GD. The absorption coefficient is calculated in two ways (as discussed above with regard to Figure 3): as the average *apparent* value for the thickness of material tested (i.e., the slope of a line from zero thickness up to the point on the curve for that thickness; solid line, left scale), and as the *marginal* value based on local slope of the curve (dotted line, left scale). As indicated, for a thin sample (thickness  $0.1\text{mm}$ ), the absorption coefficient is about  $5000\text{m}^{-1}$ , and the value drops rapidly as the sample gets thicker. The marginal value of the absorption coefficient drops off somewhat faster than the apparent value and achieves a lower value at  $S=3\text{mm}$ . Also shown in Figure 7 is the fraction of total energy attenuated (reflected and absorbed) as a function of the sample thickness. As indicated, about two-thirds of the energy is attenuated within the first  $0.33\text{mm}$ , and the apparent absorption coefficient for that thickness is about  $3200\text{m}^{-1}$ . The significance is that whereas tests with larger thicknesses of material might imply a value of  $a$  near  $1000\text{m}^{-1}$ , most of the energy has already been absorbed at smaller thickness, where the apparent value of  $a$  is much larger.

There are two ramifications of the results presented above. First, for spectral measurements, it is important to measure the transmission spectra in a wide enough range of wavelengths. Second, for polymers of interest in fire research, the transmission of IR is not described well by Bouguer's law using a constant value of the absorption coefficient for broadband radiation. These are discussed below.

The required spectral range for accurate description of the absorption of radiant energy depends upon both the blackbody source temperature and the particular spectra of the polymer (as illustrated in Figure 4). To investigate the influence of the former, Figure 8 shows the calculated fraction of the

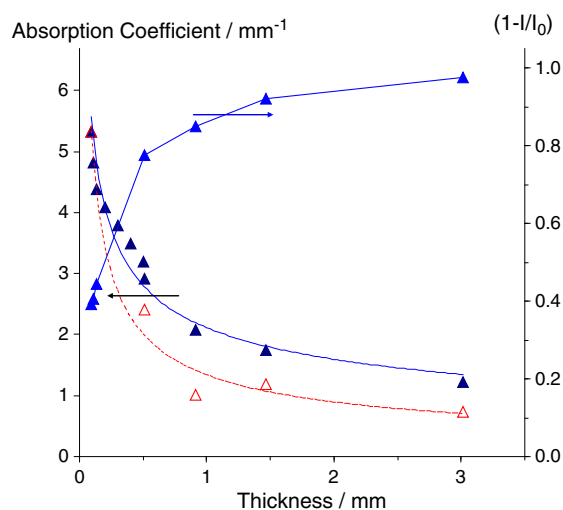


Figure 7. Apparent absorption coefficient (left scale, solid line) of black poly(methyl methacrylate) for broadband infrared as a function of thickness and the marginal absorption coefficient (left scale, dotted line), both from the National Institute of Standards and Technology gasification device. Also shown (right scale) is the fraction of light attenuated,  $[1 - (I/I_0)]$ , for each sample thickness.

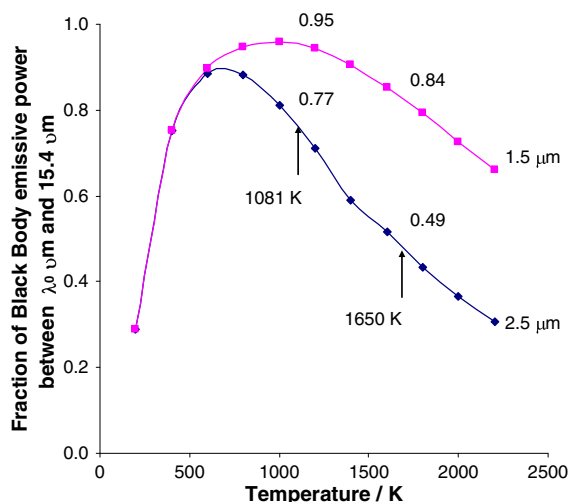


Figure 8. Fraction of blackbody emissive power between 1.5 and 15.1  $\mu\text{m}$  or 2.5 and 15.1  $\mu\text{m}$  as a function of source temperature.

blackbody emissive power [1], which lies in the wavelength range of either 1.5 to 15.1  $\mu\text{m}$  or 2.5 to 15.1  $\mu\text{m}$ , as a function of the source temperature. In the case of fires, the source temperature of interest would typically be the upper-layer hot gas temperature; in the case of simulating a mass-loss experiment in a laboratory-scale sample [16,28], the source temperature would be that of the radiant heater used for the experiment. (Temperatures of 500 to 1100 K in the cone calorimeter, for example, are used to provide a flux of about 5 to 75  $\text{kW m}^{-2}$ ; i.e., changing incident fluxes typically employ different blackbody source temperatures, which could affect the absorption coefficient.) The arrows indicate the source temperatures for the NIST GD in the present work, as well as the FM Global device used in reference [16], along with the value on each curve at that temperature.

As Figure 8 shows, for a radiant source at 1081 K, about 95% of the blackbody emissive power is within the wavelength range of the NIST IS detector (with about one-half of the remaining power below 1.5  $\mu\text{m}$  and the other half above 15.1  $\mu\text{m}$ ). Figure 8 also shows the fraction of energy in the wavelength range of 2.5 to 15.1  $\mu\text{m}$ . Although it is highly dependent upon the absorption spectrum of the polymer of interest, the 2.5- $\mu\text{m}$  to 15.1- $\mu\text{m}$  spectral range would likely be insufficient for radiation from fires. Even more important than the blackbody distribution is how a spectra for a particular polymer falls within the blackbody distribution; a range acceptable for one polymer may not be for another. In some situations, it is very important to collect spectral data over as wide a range of wavelengths as possible, as has been carried out for absorptance and absorptivity measurements [29–31], or to use a broadband technique. Finally, it is important to note that even for black (Polycast) PMMA (as well as many of the other polymers discussed below), the transmittance has spectral variation (i.e., is not gray), which can affect the absorption of thermal radiation, depending upon the spectral distribution of the radiation source [29].

The present spectral technique has been applied for understanding the absorption of IR by plastic glazings for solar thermal collectors in reference [7]. In that work, transmission spectra in the wavelength range of 2.5 to 15  $\mu\text{m}$  was used to estimate the total average transmittance from a black body emitter at varying temperatures (up to 873 K). Based on the present data, it is suggested that a wider wavelength range would be desirable for that application as well. For a source at 873 K, nearly 11% of the blackbody emissive power is below 2.54  $\mu\text{m}$ . Using the present NIST IS spectral data (which are described in more detail below) for PET (e.g., Mylar), PMMA (clear, e.g., Plexiglass), and PP and integrating over either 1.5 to 15  $\mu\text{m}$  or 2.5 to 15  $\mu\text{m}$  produce the total average transmittance as listed in Table II. As indicated, the inferred value of the total average transmittance is significantly different for integration of the NIST IS data over the two spectral ranges. Hence, a wider spectral range for spectral transmission data may be required for the materials described in reference [7] for a source at 873 K.

Table II. Total average transmittance of 3-mm samples as calculated from the National Institute of Standards and Technology integrating-sphere spectral transmittance data.

Polymer	Transmittance (%)	
	2.5 to 15 $\mu$ m	1.5 to 15m
PET	0.3	3.0
PMMA (clear)	0.5	9.6
PP	4.7	13.0

The non-Bouguer's law behavior of the absorbed light for broadband sources is more problematic. It occurs, essentially, because as the incident radiation penetrates the sample, the distribution of energy is no longer that of a blackbody. That is, integration of the spectral transmittance over the blackbody energy distribution is accurate at the surface, but not at depth, where the strong lines have depleted the energy near the spectral regions of high absorption. This has been dealt with in the past through the use of multi-band models of the radiation [32]. The need to do this in sub-grid models of material burning may need to be examined, depending upon the particular material and use of the simulation, or perhaps a method based on a non-constant value of the average total absorption coefficient might be employed. The importance of multi-band treatment of the radiation or other methods of accounting for non-constant values of the absorption coefficient with thickness will be more important at high imposed heat flux, in which the effects of in-depth absorption are more pronounced.

With the detailed discussion above for POM and black PMMA, the behavior of the remaining polymers can now be interpreted. Figure 9 shows plots of  $-\ln(I/I_0)$  versus sample thickness for PS, PP, HDPE, clear PMMA, PA66, and PET, whereas Figure 10 shows these plots for HIPS, PBT, and PBT-GF. The individual plots are provided in the approximate order of increasing absorption coefficient. For reference, as in Figure 3, the fraction of incident energy which is attenuated [ $1 - (I/I_0)$ ] is shown in the right (non-linear) scale. As above, data are presented for measurements in the NIST GD ( $\Delta$  symbols, connected by lines) and in the NIST IS ( $\circ$  symbols); however, for these polymers (except PBT and PBT-GF, which have data for a variety of thicknesses), the IS data were collected only for one sample thickness near 3mm. At zero thickness, the NIST IS-measured reflectance provides the data indicated by the  $\circ$  symbol, while the real value of the index of refraction provides the data indicated by the  $\blacklozenge$  symbol.

For HDPE, PET, HIPS, PBT, and PBT-GF (as well as POM and black PMMA discussed above), the NIST GD values are relatively close to the NIST IS values, whereas for the others, there is a significant difference. As discussed above, the discrepancy is likely related to the adequacy of the spectral range of the IS measurements (1.5 to 15 $\mu$ m) for capturing the spectral properties of the particular polymer at the source temperature of the NIST GD (1081 K).

For some of the polymers, for example, PS and HDPE, the curves for  $-\ln(I/I_0)$  versus thickness are nearly linear, indicating a roughly constant value of  $a$ , whereas for the others, the slope ( $a$ ) is higher for smaller thicknesses, as was the case for POM and black PMMA above. For example, the marginal slope is about 13 times higher for a 0.5-mm-thick sample of PA66 as compared with the 3-mm sample, but only twice as high for PS. Figure 11 shows, for all of the polymers, the variation with thickness of the total average absorption coefficient (*apparent*, as discussed above). As indicated in the figure, the relatively transparent polymers (PS, PP, and HDPE) have approximately constant values of the apparent absorption coefficient  $a$ , near  $1000\text{m}^{-1}$  for 3-mm samples and 1000 to  $2000\text{m}^{-1}$  for 0.5-mm samples; that is,  $a$  is only a factor of 1 to 2 higher at 0.5mm as compared with 3mm. The remaining polymers have values of  $a$  from 1000 to  $2000\text{m}^{-1}$  at 3mm and about 3000 to  $5000\text{m}^{-1}$  at 0.5mm; typically about 3.5 times higher at 0.5mm than at 3.0mm. These values of  $a$  allow an estimate of the mean characteristic penetration depth  $l_m = 1/a$  of the radiant flux. From Figure 11,  $a$  determined from specimens 3-mm thick would imply  $l_m$  of 0.5 to 1.1mm, whereas measurements using samples 0.25-mm thick would imply  $l_m$  of 0.16 to 1mm.

For fire research, values of the total average absorption coefficient are needed for use in fire models. Unfortunately, these are shown to vary with material thickness (i.e., for broadband radiation, the

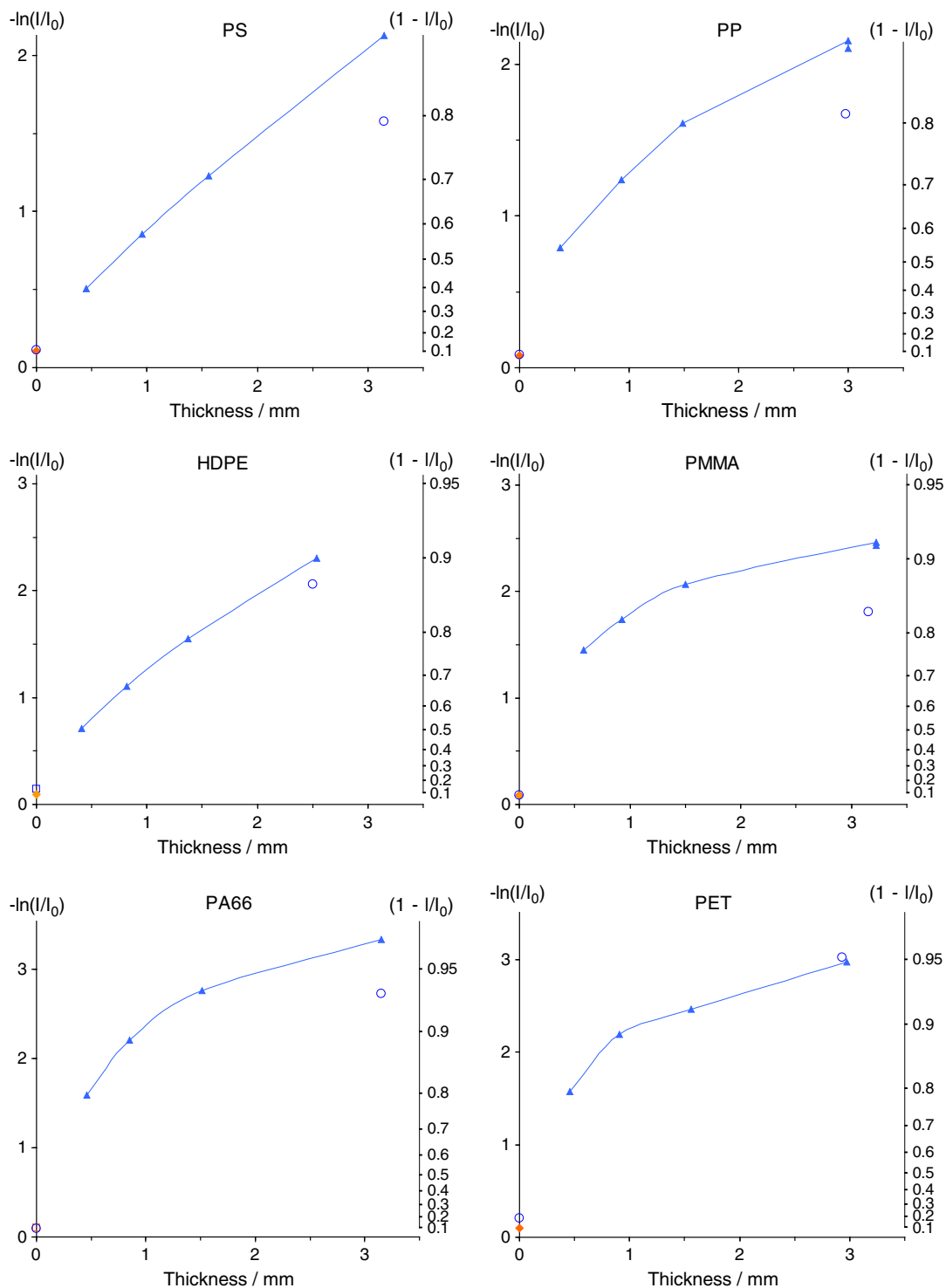


Figure 9.  $[1 - (I/I_0)]$  (right scale) and  $-\ln(I/I_0)$  (left scale) versus thickness for polystyrene (PS), polypropylene (PP), polyethylene (high density) (HDPE), poly(methyl methacrylate) (PMMA, clear), polyamide 6,6 (PA66), and poly(ethylene terephthalate) (PET), as measured in the National Institute of Standards and Technology gasification device ( $\Delta$ ) and integrating-sphere system ( $\circ$ ), at a source temperature of 1081 K.

materials do not follow Bouguer's law). Nonetheless, at the material thicknesses in which most of the energy are absorbed, the values of  $a$  are quite high. For example, Figure 12 shows the apparent

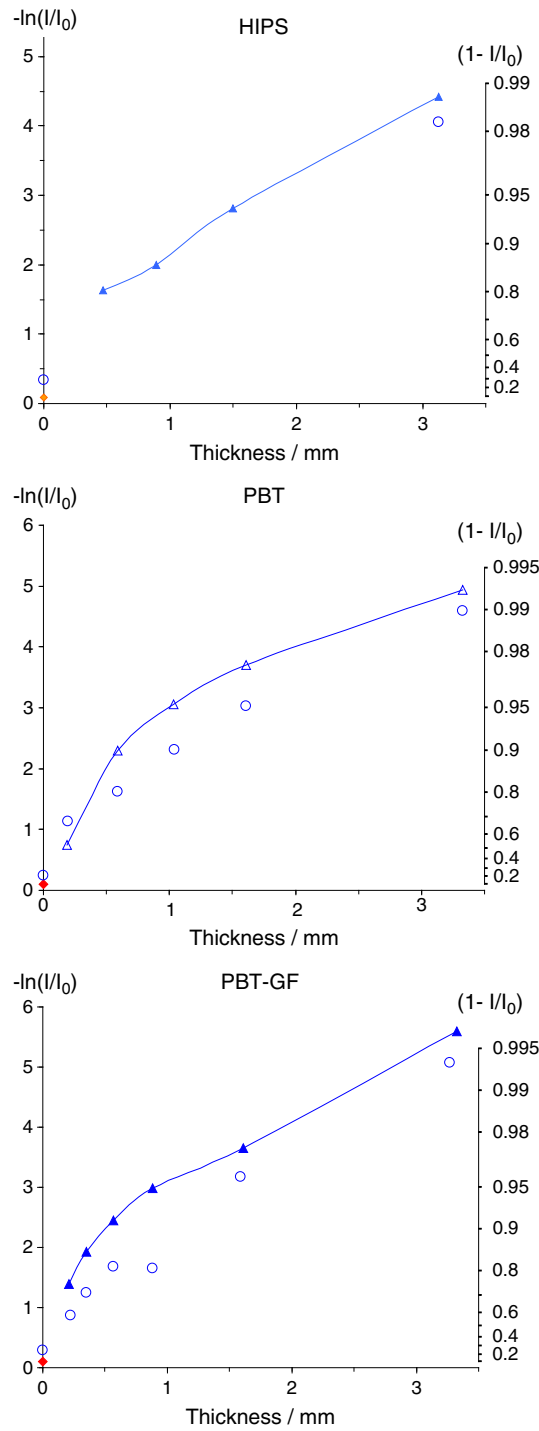


Figure 10.  $[1 - (I/I_0)]$  (right scale) and  $-\ln(I/I_0)$  (left scale) versus thickness for polystyrene (high impact) (HIPS), poly(butylene terephthalate) (PBT), and poly(butylene terephthalate) with glass fiber (PBT-GF), measured in the National Institute of Standards and Technology gasification device ( $\Delta$ ) and integrating-sphere system ( $\circ$ ), at a source temperature of 1081 K.

absorption coefficient as a function of the fraction of incident energy absorbed (based on the measured transmissivity in the NIST GD, as shown in Figures 9 and 10). The inset in Figure 12 shows the apparent value of  $a$  at a thickness in which 80% of the incident energy has been absorbed. For all the polymers tested here, except for the relatively transparent polymers (PS, HDPE, PP, and clear

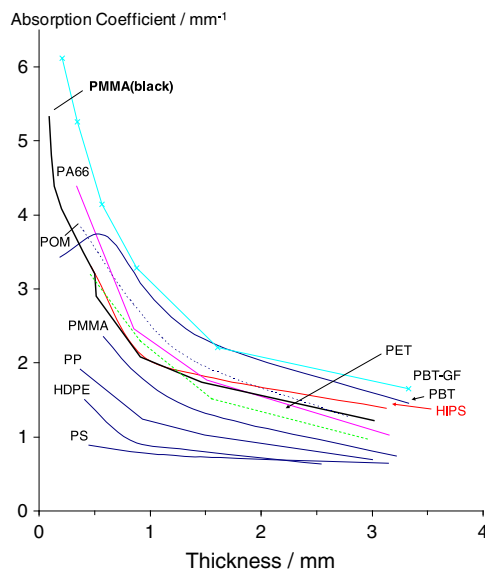


Figure 11. Total average absorption coefficient (apparent) as a function of sample thickness for the various polymers, at a source temperature of 1081 K. PMMA, poly(methyl methacrylate); PET, poly(ethylene terephthalate); PBT, poly(butylene terephthalate); PBT-GF, poly(butylene terephthalate) with glass fiber; HIPS, polystyrene (high impact).

PMMA), 80% of the energy has already been absorbed at a depth in which the absorption coefficient is 2600 to 6000  $\text{m}^{-1}$ . For example, for black PMMA, at a depth of 0.4 mm, 64% of the energy has been absorbed, and the apparent value of  $a$  is 3500  $\text{m}^{-1}$ , whereas at a depth of 0.51 mm, 78% of the energy has been absorbed, and the apparent value of  $a$  is 2900  $\text{m}^{-1}$ . These values of  $a$  are significantly higher than one might use based on broadband measurements of transmittance for thicker specimens of polymer (e.g., as in Figure 11 for 2-mm to 3-mm-thick samples).

Given the IR absorption properties of the polymers described above, the influence of absorption coefficient on the burning behavior can be inferred. Using the simulated results in reference [20] for the modeled thermoplastic, values of  $a$  between 1000 and 6000  $\text{m}^{-1}$  will have a minor effect on the shape of the mass loss versus time curve. Likewise, this increase in  $a$  lowers the average burning rate by about 9% at an external heat flux of 21  $\text{kW m}^{-2}$  and raises it by about 4% at 200  $\text{kW m}^{-2}$ , whereas for (50, 100, or 150)  $\text{kW m}^{-2}$ , the effect is only a few percentage. The ignition time is more strongly affected: lowering  $a$  from 6000 to 1000  $\text{m}^{-1}$  increases the ignition time by a factor of 3 at 200  $\text{kW m}^{-2}$  and 1.5 at 50  $\text{kW m}^{-2}$ . Of course, the relative effects will differ if the polymer properties vary from those in reference [20]. It is also noteworthy that the measured broadband absorption coefficient for black PMMA in the present work (as indicated in Figure 7) is outside the range of values (333 to 2000  $\text{m}^{-1}$ ) found in the literature by Bal and Rien [18], when a sample thickness is considered in which most of the energy is absorbed.

From a practical perspective, it is important to note that the present measurements were taken at near room temperature. Any potential changes in the optical properties of the polymers with temperature increase are not accounted for. Also, with polymer decomposition, small bubbles of gaseous products often form in the polymer just below the surface. These would have the effect of scattering light and increasing the effective absorption coefficient. Hence, the actual absorption of incident light may be even higher than expected based on the present measurements.

The reflectance of the materials for broadband radiation from a source at 1081 K was also determined in the NIST IS system, as described above. The present measurements made in the NIST GD do not provide the reflectance; although they could be obtained by extrapolating the results to zero thickness, this is not carried out here because measurements with sufficiently thin samples were not available. Nonetheless, the data in Figures 9 and 10 from the NIST GD are consistent with the values of  $\rho$  obtained in the NIST IS (plotted in those figures at  $S=0$ ). Table III lists the values of  $\rho$  for each polymer (in order of increasing reflectance) as obtained in the NIST IS. For some polymers (black PMMA, POM, PBT, and PBT-GF), the reflectance was measured for the entire set of polymer

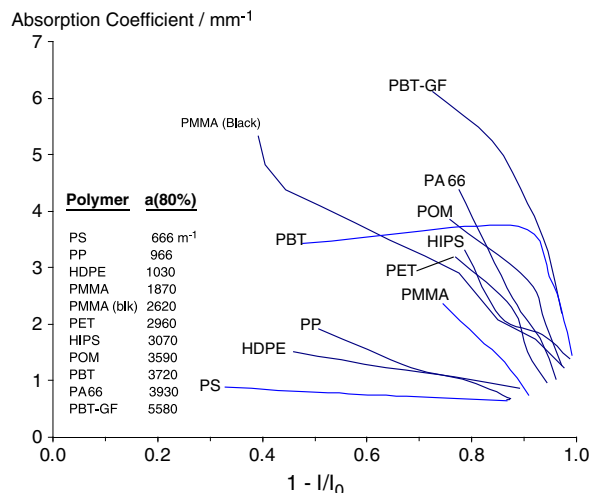


Figure 12. Total average absorption coefficient (apparent) versus the fraction of incident energy absorbed  $[1 - (I/I_0)]$  for the tested polymers, at a source temperature of 1081 K. PMMA, poly(methyl methacrylate); PS, polystyrene; PP, polypropylene; HDPE, polyethylene (high density); PET, poly(ethylene terephthalate); HIPS, polystyrene (high impact); POM, poly(oxymethylene); PBT, poly(butylene terephthalate); PA66, polyamide 6,6; PBT-GF, poly(butylene terephthalate) with glass fiber.

thicknesses. For those polymers, the thinner samples had larger measured reflectance (because of the reflecting off of both the front and back surfaces, with little absorption while traversing the small sample thickness). Hence, for each of these polymers, the NIST IS-measured reflectance is presented only for the thickest sample, so as to represent reflectance from the front surface only. Also shown in the table are the values of  $\rho$  estimated from Equation 8, using the index of refraction (in the visible) obtained from literature sources. As indicated, based on the index of refraction, the reflectance would be around 4% to 5% for all the polymers. The NIST IS data, however, indicate that for some of the polymers, (HDPE, PET, PBT, PBT-GF, and HIPS), the reflectance is higher, varying from about 7% to 15%.

### 5. CONCLUSIONS

Two experimental methods were investigated for obtaining the absorption coefficient of materials for use in fire research. The first is a broadband method that uses a radiant heater, together with a broadband thermal detector (e.g., the NIST GD or cone calorimeter, FM Global FPA). The second is a spectral technique that measures the reflectance or transmittance spectra (e.g., using the NIST IS

Table III. Total average reflectance of polymers, estimated based on the index of refraction and measured in the NIST IS.

Polymer	Thickness (mm)	$n_f$	Reflectance $\rho$	
			$n_f$ -based	NIST IS
PMMA (black)	3.00	1.49	0.0386	0.037
PP	2.97	1.49	0.0387	0.041
PMMA (clear)	3.15	1.49	0.0386	0.041
PA66	3.15	1.56	0.0485	0.046
POM	2.80	1.48	0.0375	0.051
PS	3.15	1.59	0.0518	0.054
HDPE	2.50	1.54	0.0420	0.070
PET	2.93	1.58	0.0499	0.097
PBT	3.33	1.55	0.0465	0.117
PBT-GF	3.27	1.55	0.0465	0.134
HIPS	3.13	1.52	0.0400	0.154

system). Both techniques have been used to measure the transmittance as a function of thickness, for 11 common thermoplastics, from which the average total absorption coefficient was inferred. For the polymers HDPE, PET, PBT, PBT-GF, HIPS, PMMA (black), and POM, the broadband method gives results for the transmittance as a function of sample thickness reasonably close to those obtained by measuring the transmittance spectra using the NIST IS and integrating the transmittance over the blackbody energy distribution at the temperature of the heater.

Using the spectral method, an FTIR spectral range of 2.5 to 15.1  $\mu\text{m}$  was found to be insufficient for characterizing these materials with respect to IR transmission, especially for the thicker samples and could lead to misleading results; moreover, a spectral range of 1.5 to 15.1  $\mu\text{m}$  was acceptable for POM, black PMMA, HDPE, HIPS, PBT, and PBT-GF (although this will vary with the material and the source temperature). Also, for broadband transmissivity estimates for solar thermal collector glazings, the wavelength range of spectral transmittance measurements must be wide enough to accurately characterize typical materials. Many of the polymers of the present study have strong resonances in the wavelength range typical of fires. Hence, the absorption of thermal radiation will vary with the spectral distribution of the source, because of temperature or strong emitting species (e.g.,  $\text{H}_2\text{O}$  or  $\text{CO}_2$ ).

For use in pyrolysis simulations for fire research, the average total absorption coefficient is desired, but for broadband radiation, the average absorption coefficient of most of these materials (all but PE and PS) was not constant with thickness. The average total absorption coefficient (marginal) often varied by nearly an order of magnitude for sample thicknesses between 0.2 and 3 mm. Nonetheless, for the present polymers (except for the most transparent polymers HDPE, PS, and PP), most of the energy is absorbed within the first 0.5 mm, and the apparent absorption coefficient for that thickness is fairly large. For the depth at which 80% of the incident energy is absorbed, the apparent value of the total average absorption coefficient ranges from 1000 to 6000  $\text{m}^{-1}$  for the polymers tested. With either the broadband or spectral technique, the present results highlight the importance of conducting the transmission measurements on sample thicknesses of the order of the mean penetration depth (or thinner), so that a representative value of the absorption coefficient can be obtained.

The average total reflectance of the polymers was also calculated from the spectral reflectance measured with the NIST IS (IS) system. For most of the polymers, the average total reflectance for a source at 1081 K was 4% to 5%, but for others, it ranged from 7% to 15%.

There may be specific uses of pyrolysis models with semi-transparent polymers in which multi-band treatment of the radiation heat transfer may be necessary. For example, at very high heat flux, the ignition time is very sensitive to the value of the absorption coefficient; hence, accurate prediction of the ignition time at high flux may require spectral transmittance data for the polymer, as well as multi-line treatment of the radiation transfer.

#### ACKNOWLEDGEMENTS

The authors thank John de Ris and Mohammed Khan at FM Global and Stanislov Stoliarov and Rich Lyon of the FAA Technical Center, for the helpful conversations and for sending specimens of their material. We are grateful to Takashi Kashiwagi and Ken Steckler at NIST, who performed the experiments in the NIST GD and provided valuable insight, and Paul Fuss of the BATF, who helped with some initial exploratory FTIR measurements.

#### REFERENCES

1. Siegel R, Howell JR. *Thermal Radiation Heat Transfer*. Hemisphere Pub. Corp.: Washington, 1981.
2. Katzoff S. *Symposium on Thermal Radiation of Solids*. NASA SP-55. National Aeronautics and Space Administration: Washington, D.C., 1965.
3. Progelhof RC, Throne JL. Determination of optical properties from transmission measurements. *Applied Optics* 1971; **10**(11):2548–2549.
4. Progelhof RC, Franey J, Haas TW. Absorption coefficient of unpigmented poly(methyl methacrylate), polystyrene, polycarbonate, and poly(4-methylpentene-1) sheets. *Journal of Applied Polymer Science* 1971; **15**(7):1803–1807.
5. Progelhof RC, Quintiere JG, Throne JL. Temperature distribution in semitransparent plastic sheets exposed to symmetric, unsymmetric, and pulsed radiant heating and surface cooling. *Journal of Applied Polymer Science* 1973; **17**(4):1227–1252.
6. Progelhof RC, Throne JL. Predicting radiant energy transmission through polymer sheets. *Polymer Engineering and Science* 1974; **14**(11):760–763.

7. Tsilingiris PT. Comparative evaluation of the infrared transmission of polymer films. *Energy Conversion and Management* 2003; **44**(18):2839–2856.
8. Kashiwagi T. Radiative ignition mechanism of solid fuels. *Fire Safety Journal* 1981; **3**(3):185–200.
9. Kashiwagi T. Polymer combustion and flammability—role of the condensed phase. *Proceedings of the Combustion Institute* 1994; **25**:1423–1437.
10. Sohn Y, Baek SW, Kashiwagi T. Transient modeling of thermal degradation in non-charring solids. *Combustion Science and Technology* 1999; **145**(1–6):83–108.
11. Drysdale D. *An Introduction to Fire Dynamics*. John Wiley and Sons: Chichester, England, 1998.
12. Lautenberger C. *A Generalized Pyrolysis Model for Combustible Solids*. Ph.D. dissertation, Univ. of California, Berkeley; Berkeley, CA, 2010; 1–370.
13. Hallman JR, Welker JR, Sliepcevich CM. Ignition times for polymers. *Polymer—Plastics Technology and Engineering* 1976; **6**(1):1–56.
14. Nicolette VV, Erickson KL, Vembe BE. Numerical simulation of decomposition and combustion of organic materials. *Proceedings of Interflam 2004, 10th International Conference on Fire Science and Engineering*, Interscience Communications Ltd: London, 2004.
15. Stoliarov SI, Crowley S, Lyon RE, Linteris GT. Prediction of the burning rates of non-charring polymers. *Combustion and Flame* 2009; **156**(5):1068–1083.
16. Jiang FH, de Ris JL, Khan MM. Absorption of thermal energy in PMMA by in-depth radiation. *Fire Safety Journal* 2009; **44**(1):106–112.
17. Saito K, Delichatsios MA, Venkatesh S, Alpert RL. *Measurement and Evaluation of Parameters Affecting the Preheating and Pyrolysis of Noncharring Materials*, Paper Prepared for Presentation at the Fall Technical Meeting, Eastern Section The Combustion Institute: Clearwater Beach, FL, December 1988.
18. Bal N, Rein G. Numerical investigation of the ignition delay time of a translucent solid at high radiant heat fluxes. *Combustion and Flame* 2011; ACCEPTED doi:10.1016/j.combustflame.2010.10.014.
19. Girods P, Bal N, Biteau H, Rein G, Torero JL. *Comparison of Pyrolysis Behavior Results between the Cone Calorimeter and the Fire Propagation Apparatus Heat Sources*. International Association for Fire Safety Science: Boston, MA, 2011; 625–636.
20. Linteris G. Numerical simulations of thermoplastic pyrolysis rate: effects of property variations. *Fire and Materials* 2010; ACCEPTED doi:10.1002/fam.1066.
21. McGrattan KB, Klein B, Hostikka S, Floyd J. *Fire Dynamics Simulator (Version 5) User's Guide*. NIST Special Publication 1019-5. National Institute of Standards and Technology: Gaithersburg, MD, 2007.
22. Stoliarov SI, Lyon RE. *Thermo-kinetic Model of Burning*. Federal Aviation Administration Technical Note DOT/FAA/AR-TN08/17. Federal Aviation Administration: Atlantic City, NJ, 2008.
23. Austin PJ, Buch RR, Kashiwagi T. Gasification of silicone fluids under external thermal radiation. Part I. Gasification rate and global heat of gasification. *Fire and Materials* 1998; **22**(6):221–237.
24. Hanssen L. Integrating-sphere system and method for absolute measurement of transmittance, reflectance, and absorptance of specular samples. *Applied Optics* 2001; **40**(19):3196–3204.
25. Chenault DB, Snail KA, Hanssen LM. Improved integrating-sphere throughput with a lens and nonimaging concentrator. *Applied Optics* 1995; **34**(34):7959–7964.
26. Stoliarov SI, Walters RN. Determination of the heats of gasification of polymers using differential scanning calorimetry. *Polymer Degradation and Stability* 2008; **93**(2):422–427.
27. Kempel F, Schartel B, Hofmann A, Linteris GT, Lyon RE, Walters RN, Stoliarov SI. Prediction of the mass loss rate of polymer materials: impact of residue formation. *Combustion and Flame* 2011; to be submitted.
28. Twilley WH, Babrauskas V. *User's Guide for the Cone Calorimeter*. SP-745, National Institute of Standards and Technology: Gaithersburg, MD, 1988.
29. Hallman JR. Ignition characteristics of plastics. Ph.D. Dissertation, University of Oklahoma: Norman, OK, 1971; 1–364.
30. Wesson HR, Welker JR, Sliepcevich CM. Piloted ignition of wood by thermal radiation. *Combustion and Flame* 1971; **16**(3):303–310.
31. Forsth M, Roos A. Absorptivity and its dependence on heat temperature and degree of thermal breakdown. *Fire and Materials* 2011; (Article in Press) doi:10.1016/S0010-2180(71)80101-3.
32. Manohar SS, Kulkarni AK, Thynell ST. In-depth absorption of externally incident radiation in nongray media. *Journal of Heat Transfer—Transactions of the ASME* 1995; **117**(1):146–151.